ISA Transactions 52 (2013) 365–374

Contents lists available at SciVerse ScienceDirect

ISA Transactions

journal homepage: www.elsevier.com/locate/isatrans

Research Article

Active disturbance rejection control for fractional-order system

Mingda Li [a,*], Donghai Li [b,1], Jing Wang [a,2], Chunzhe Zhao [b,c,3]

[a] Engineering Research Institute, University of Science and Technology Beijing, No. 30 Xueyuan Road, Haidian District, Beijing 100083, China
[b] State Key Lab of Power Systems Dept. of Thermal Engineering, Tsinghua University, Haidian District, Beijing 100084, China
[c] School of Computer Science and Engineering, Chongqing Three Gorges University, Chongqing 404000, China

ARTICLE INFO

Article history:
Received 3 July 2012
Received in revised form
1 December 2012
Accepted 2 January 2013
Available online 8 February 2013
This paper was recommended for publication by Dr. Y. Chen

Keywords:
Fractional-order system
Active disturbance rejection control
Extended state observer
Stability

ABSTRACT

Fractional-order proportional–integral (PI) and proportional–integral–derivative (PID) controllers are the most commonly used controllers in fractional-order systems. However, this paper proposes a simple integer-order control scheme for fractional-order system based on active disturbance rejection method. By treating the fractional-order dynamics as a common disturbance and actively rejecting it, active disturbance rejection control (ADRC) can achieve the desired response. External disturbance, sensor noise, and parameter disturbance are also estimated using extended state observer. The ADRC stability of rational-order model is analyzed. Simulation results on three typical fractional-order systems are provided to demonstrate the effectiveness of the proposed method.

1. Introduction

Fractional-order system and control have been studied by many researchers in the past decade because fractional calculus can model real-world phenomena more precisely [1,2]. Some fractional-order models, such as heating–furnace [3], gas–turbine [4,5], and heat solid models [6] are obtained using system identification methods. Compared with integer-order model, the exact fractional-order model of a process usually has a complicated structure, which could be reduced and approximated to a simple one [7,8]. Otherwise, fractional-order controllers, as a generalization of traditional integer-order controllers, have been suggested to enhance the performance of control systems [9,10]. Some fractional-order controllers have been introduced in the literature such as the fractional PID controller [3,7,8,11–19], the fractional lead–lag compensator [20], different generations of the CRONE controllers [21–24], and optimal fractional controllers [25]. It is particularly pointed out that Ref. [26,27] proposed a new method to control single-link lightweight flexible manipulators in the presence of changes in the load. The nonlinear effects have been compensated and the system transfer function is reduced to a double integrator. The proposed method in this paper is also a little similar to that.

For fractional-order model, fractional-order controller can be naturally considered as the best controller. However, the active disturbance rejection control (ADRC), proposed as an alternative paradigm for control system design, offers a novel perspective [28,29]. The active disturbance rejection concept originated from Han [30], and full account of ADRC is provided in Ref. [31]. The original ADRC contains tracking differentiator, nonlinear PID, and extended state observer (ESO). Bandwidth-parameterization method is proposed to improve ADRC for easy tuning [32]. Stability [33–35] and frequency response [36] are also researched. ADRC has been applied to DSP-based power converter [37], delay system [38], motion control [39–42], hysteretic system [43], high-performance turbofan engines [44], flight control [45], interconnected power system [46], decoupling [47], micro-electro-mechanical systems (MEMS) gyroscopes [48,49], noncircular turning process [50], and coordinated robust nonlinear boiler–turbine–generator control system [51].

Motivated by these applications, a novel approach named fractional-order dynamics rejection scheme is proposed for fractional-order system based on active disturbance rejection method. By treating the fractional-order dynamics as a common disturbance and actively rejecting it, ADRC achieves the desired response, and ESO estimates effectively the external disturbance, sensor noise, and parameter disturbance. Stability analysis

* Corresponding author. Tel.: +8613581819826.
E-mail addresses: inventorlmd@gmail.com (M. Li), lidongh@mail.tsinghua.edu.cn (D. Li), wangj@nercar.ustb.edu.cn (J. Wang), zcz@amss.ac.cn (C. Zhao).
[1] Tel.: +86 10 62782272
[2] Tel.: +86 10 62332598 6306.
[3] Tel.: +8613699252268.

0019-0578/$ - see front matter © 2013 ISA. Published by Elsevier Ltd. All rights reserved.
http://dx.doi.org/10.1016/j.isatra.2013.01.001

demonstrates that the fractional-order system can be controlled by ADRC, and simulation results show satisfactory system response.

This paper is organized as follows: A brief introduction of the fractional-order system is described in Section 2. Section 3 presents the ADRC and its stability analysis. Section 4 demonstrates the proposed algorithm of some examples, including a heating–furnace, gas–turbine, and heat solid models. Conclusions are given in Section 5.

2. Fractional-order systems

The Grünwald–Letnikov's definition is the most popular definition of fractional-order derivatives for fractional-order control and its application; it has the form,

$$\mathcal{D}^{\alpha}f(t)=\frac{d^{\alpha}f(t)}{dt^{\alpha}}=\lim_{h\to 0}\frac{1}{h^{\alpha}}\sum_{j=0}^{\infty}(-1)^{j}\binom{\alpha}{j}f(t-jh),\ \alpha\in N \tag{1}$$

where $(-1)^{j}\binom{\alpha}{j}$ is the usual notation for binomial coefficients, such as $(1-z)^{\alpha}$.

The first-order derivative of function $f(t)$, denoted by $D^1f(t)$, is defined as

$$\mathcal{D}^{1}f(t)=\frac{df(t)}{dt}=\lim_{h\to 0}\frac{f(t)-f(t-h)}{h} \tag{2}$$

Obviously, the fractional-order derivative is important for long-term conditions. However, the integer-order derivative is only relevant for the current moment. The fractional-order derivative characteristic makes the system response slow and sensitive to disturbance.

The Laplace transform of the Grünwald–Letnikov fractional-order derivative is given by

$$\mathcal{L}[\mathcal{D}^{\alpha}f(t)]=s^{\alpha}F(s) \tag{3}$$

where zero initial condition is considered.

A general single-input–single-output fractional-order system can be expressed as

$$\begin{aligned}&a_n y^{(\alpha_n)}(t)+a_{n-1}y^{(\alpha_{n-1})}(t)+\cdots+a_1y^{(\alpha_1)}(t)+a_0y(t)\\&=b_m u^{(\beta_m)}(t)+b_{m-1}u^{(\beta_{m-1})}(t)+\cdots b_1u^{(\beta_1)}(t)+b_0u(t)\end{aligned} \tag{4}$$

The transfer function is represented by

$$G(s)=\frac{B(s)}{A(s)}=\frac{b_m s^{\beta_m}+b_{m-1}s^{\beta_{m-1}}+\cdots b_1s^{\beta_1}+b_0}{a_n s^{\alpha_n}+a_{n-1}s^{\alpha_{n-1}}+\cdots+a_1s^{\alpha_1}+a_0} \tag{5}$$

where $\alpha_n>\alpha_{n-1}>\cdots>\alpha_1>0$ and $\beta_m>\beta_{m-1}>\cdots>\beta_1>0$ are arbitrary positive rational numbers. Assumption is made that $a_i,b_j(i=0,1,\cdots n.j=0,1,\cdots n)$ are positive, and $\alpha_n>\beta_m$.

All rational numbers can be expressed as a ratio of two integers. Eq. (5) is therefore rewritten as follows:

$$\begin{aligned}H(s)=\frac{h_2(s)}{h_1(s)}b&=\frac{b\left(h_{2m_2}s^{\frac{m_2}{q}}+h_{2(m_2-1)}s^{\frac{m_2-1}{q}}+\cdots+1\right)}{s^{\frac{m_1}{q}}+h_{1(m_1-1)}s^{\frac{m_1-1}{q}}+\cdots+h_{11}s^{\frac{1}{q}}+h_{10}}\\&=\frac{b\left(\sum_{i=1}^{m_2}h_{2i}s^{\frac{i}{q}}+1\right)}{s^{\frac{m_1}{q}}+\sum_{i=0}^{m_1-1}h_{1i}s^{\frac{i}{q}}},\end{aligned} \tag{6}$$

where $q>0$, $m_1>0$, $m_2\geq 0$ are integers, $b\neq 0$, and $m_1\geq m_2$. Obviously, this fractional-order system is a commensurate-order system. In this paper, the fractional-order systems are assumed to be bounded-input bounded-output (BIBO) stable according to the Matignon theorem [52].

For the above-mentioned fractional-order systems, Tavakoli-Kakhki proposed a reduction technique to approximate these systems into three simple structures [7]. Without loss of generality, we consider the three most common types of fractional-order dynamic systems under the above conditions as follows:

$$\text{TypeI}.\ a_1y^{(\alpha_1)}+a_0y=b_0u \tag{7a}$$

$$\text{TypeII}.\ a_2y^{(\alpha_2)}+a_1y^{(\alpha_1)}+a_0y=b_0u \tag{7b}$$

$$\text{TypeIII}.\ a_3y^{(\alpha_3)}+a_2y^{(\alpha_2)}+a_1y^{(\alpha_1)}+a_0y=b_1u^{(\beta_1)}+b_0u,\ \alpha_3\geq\beta_1 \tag{7c}$$

In the zero initial condition, the transfer functions are

$$G_{\mathrm{I}}(s)=\frac{b_0}{a_1s^{\alpha_1}+a_0} \tag{8a}$$

$$G_{\mathrm{II}}(s)=\frac{b_0}{a_2s^{\alpha_2}+a_1s^{\alpha_1}+a_0} \tag{8b}$$

$$G_{\mathrm{III}}(s)=\frac{b_1s^{\beta_1}+b_0}{a_3s^{\alpha_3}+a_2s^{\alpha_2}+a_1s^{\alpha_1}+a_0} \tag{8c}$$

3. Active disturbance rejection control

The prevailing control scheme for fractional-order system is the fractional-order controller, which achieves theoretical effectiveness and completeness but must be approximated to high integer-order differential form and is difficult to apply to ready-made manufacturing line. The current research proposes an integer-order control scheme, which considers the fractional-order dynamics as a common disturbance to the desired integer-order dynamics and actively rejects this disturbance to present an integer-order system that is a single/double integrator. ESO is implemented in which the fractional-order dynamics are treated as a disturbance and is canceled. Then, the fractional-order system is reduced to a unit gain single/double integrator, which can be easily controlled by a proportional or proportional–derivative (PD) controller. To explain the ADRC/ESO clearly, the second-order ADRC/third-order ESO is described as a Type II system in this section. The general parameterization of n-order ADRC and ESO was proposed by Gao [32].

3.1. Fractional-order dynamics rejection scheme

For Type II system, the external disturbance, denoted by w, is also considered. Eq. (7b) can be rewritten as

$$a_2y^{(\alpha_2)}+a_1y^{(\alpha_1)}+a_0y=w+b_0u \tag{9a}$$

where y and u are the output and input, respectively. Referring to Eqs. (6) and (9a) is equivalent to

$$y^{(\alpha_2)}+\frac{a_1}{a_2}y^{(\alpha_1)}+\frac{a_0}{a_2}y=\frac{1}{a_2}w+\frac{b_0}{a_2}u \tag{9b}$$

Eq. (9b) can be rewritten as

$$\begin{aligned}\ddot{y}&=-y^{(\alpha_2)}-\frac{a_1}{a_2}y^{(\alpha_1)}-\frac{a_0}{a_2}y+\ddot{y}+\frac{1}{a_2}w+\frac{b_0}{a_2}u-b_eu+b_eu\\&=\left[-y^{(\alpha_2)}-\frac{a_1}{a_2}y^{(\alpha_1)}-\frac{a_0}{a_2}y+\ddot{y}+\frac{1}{a_2}w+\left(\frac{b_0}{a_2}-b_e\right)u\right]+b_eu\\&=f+b_eu\end{aligned} \tag{10}$$

where

$$f=-y^{(\alpha_2)}-\frac{a_1}{a_2}y^{(\alpha_1)}-\frac{a_0}{a_2}y+\ddot{y}+\frac{1}{a_2}w+\left(\frac{b_0}{a_2}-b_e\right)u$$

where, f is referred to as the generalized disturbance because it represents the fractional-order dynamics $-y^{(\alpha_2)}-(a_1/a_2)y^{(\alpha_1)}$, the external disturbance w, and the unknown internal dynamics $-(a_0/a_2)y+\ddot{y}+((b_0/a_2)-b_e)u$.

From Eq. (10), if knowledge of (b_0/a_2) is given, b_e can be tuned near (b_0/a_2). It has been proved that b_e is very robust in active disturbance rejection based control system [25,39].

3.2. Extended state observer

Define $h = \dot{f}$, the state equation form of Eq. (10) is

$$\begin{cases} \begin{bmatrix} \dot{x}_1 \\ \dot{x}_2 \\ \dot{x}_3 \end{bmatrix} = \begin{bmatrix} 0 & 1 & 0 \\ 0 & 0 & 1 \\ 0 & 0 & 0 \end{bmatrix} \begin{bmatrix} x_1 \\ x_2 \\ x_3 \end{bmatrix} + \begin{bmatrix} 0 \\ b_e \\ 0 \end{bmatrix} u + \begin{bmatrix} 0 \\ 0 \\ 1 \end{bmatrix} h \\ y = \begin{bmatrix} 1 & 0 & 0 \end{bmatrix} \begin{bmatrix} x_1 \\ x_2 \\ x_3 \end{bmatrix} \end{cases} \tag{11}$$

where $x_3 = f$ is an augmented state and f can be estimated by ESO as

$$\begin{cases} \begin{bmatrix} \dot{z}_1 \\ \dot{z}_2 \\ \dot{z}_3 \end{bmatrix} = \begin{bmatrix} 0 & 1 & 0 \\ 0 & 0 & 1 \\ 0 & 0 & 0 \end{bmatrix} \begin{bmatrix} z_1 \\ z_2 \\ z_3 \end{bmatrix} + \begin{bmatrix} 0 \\ b_e \\ 0 \end{bmatrix} u + L(y - \hat{y}) \\ \hat{y} = \begin{bmatrix} 1 & 0 & 0 \end{bmatrix} \begin{bmatrix} z_1 \\ z_2 \\ z_3 \end{bmatrix} \end{cases} \tag{12}$$

where $L = \begin{bmatrix} \beta_1 & \beta_2 & \beta_3 \end{bmatrix}^T$ is the observer gain vector. Using the bandwidth-parameterization method, all observer poles can be placed at $-\omega_o$, which is the observer bandwidth, and

$$L = \begin{bmatrix} 3\omega_o & 3\omega_o^2 & \omega_o^3 \end{bmatrix}^T \tag{13}$$

Sensor noise, sampling rate, and state-space model are important in designing ESO. A perfectly tuned ω_o must be larger than the state frequency to estimate effectively the state and disturbance. It must also be smaller than the frequency of the sensor noise, which should be filtered out and can be easily realized by the limited sampling rate. By adopting a properly designed and well-tuned ESO, outputs y and $\dot{y}$ and disturbance f can be estimated precisely. The second model in Section 4.4 is taken for example. Parameters b_e and ω_c are fixed, and ω_o is set as 10, 20, 50, 100, 200 and 500. The system responses with different ω_o are shown in Fig. 2. The little ω_o makes the ESO track slowly and the big ω_o amplifies the sensor noise.

3.3. Control algorithm

The ESO outputs track y, $\dot{y}$, and f. Denoting $z_1 = \hat{y}$, $z_2 = \hat{\dot{y}}$, and $z_3 = \hat{f}$, the control law is chosen as

$$u = \frac{-\hat{f} + u_0}{b_e} \tag{14}$$

Therefore, Eq. (10) becomes $\ddot{y} = f - \hat{f} + u_0$. Ignoring estimation error when $t \to \infty$, the Type II system is reduced to a unit gain double integrator, i.e.,

$$\ddot{y} = f - \hat{f} + u_0 \approx u_0 \tag{15}$$

which can be easily controlled by a PD controller

$$u_0 = k_p(r - \hat{y}) + k_d(-\hat{\dot{y}}) \tag{16}$$

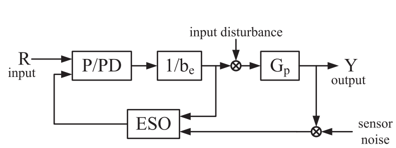

Fig. 1. Common ADRC system.

where r is the set point. $-\hat{\dot{y}}$ is used instead of $\dot{r} - \hat{\dot{y}}$ to avoid the $\dot{r}$ pulse. Thus, from the condition discussed above, Eq. (15) is rewritten as

$$\ddot{y} = k_p(r - y) + k_d(-\dot{y}) \tag{17}$$

The closed-loop system transfer function is

$$G(s) = \frac{k_p}{s^2 + k_d s + k_p} \tag{18}$$

which is the desired response of ADRC.

By applying the bandwidth-parameterization method, k_p and k_d are selected as $k_p = 2\omega_c$ and $k_d = \omega_c^2$, where ω_c is the controller bandwidth. A large ω_c can increase not only the response speed but also the magnitude and rate of change of the control signal. On the other hand, a small ω_c can enhance the stability. In practice, the observer bandwidth ω_o should be larger than the controller bandwidth ω_c so that the observer can follow the controller. Thus, controller bandwidth ω_c should be tuned in a wide range between the upper and the lower bounds. The upper bound is related to the control signal, operation cost, and observer bandwidth ω_o. The lower bound is related to stability margin and desired response. The second model in Section 4.4 is also taken for example. Parameters b_e and ω_o are fixed, and ω_c is set as 1, 2, 5, 10, and 20. The system responses with different ω_c are shown in Fig. 3. The little ω_c makes the system response slow and the big ω_c makes it fast. There are only red lines in figure output y, because the output y (blue line) and ESO estimation (green line) are so closed to the desired responses (red line), which are drawn at last.

The ADRC stability for a rational-order model is shown below.

3.4. Stability

Lemma 1. Let the integer $q > 0$, $P(s)$ be a polynomial with positive parameters and $Q(s)$ be a polynomial that satisfy $Q(0) > 0$ and $\deg Q(s) \le \deg P(s) + q$. If any root of $P(s)$ is not in the set $\left\{ z \middle| z \in \mathrm{C},\ -\frac{1}{2q}\pi \le \arg z \le \frac{1}{2q}\pi \right\}$, then $\kappa_0 > 0$ exists such that all roots of $\kappa s^q P(s) + Q(s)$ are outside the set $\left\{ z \middle| z \in \mathrm{C},\ -\frac{1}{2q}\pi \le \arg z \le \frac{1}{2q}\pi \right\}$ for each $\kappa > \kappa_0$.

Proof. Considering $\kappa > 0$, the roots of $\kappa s^q P(s) + Q(s)$ are identical to the roots of $s^q P(s) + \frac{1}{\kappa} Q(s)$. As the roots of a polynomial are continuously dependent on the parameters [53], and

$$\deg Q(s) \le \deg P(s) + q = \deg(s^q P(s)),$$

all roots of $s^q P(s) + \frac{1}{\kappa} Q(s)$ move toward the roots of $s^q P(s)$ correspondingly as κ increases. The roots of $s^q P(s) + \frac{1}{\kappa} Q(s)$ can be classified into two distinct groups. The first group is formed by q roots directed at the origin of the complex plain. The left root is in the second group, which moves toward the roots of $P(s)$ when κ increases. Hence, the roots in the second group are all outside the set $\left\{ z \middle| z \in \mathrm{C},\ -\frac{1}{2q}\pi \le \arg z \le \frac{1}{2q}\pi \right\}$ if κ is sufficiently large.

Therefore, the only remaining issue is to show that the roots in the first group are not in the set $\left\{ z \middle| z \in \mathrm{C},\ -\frac{1}{2q}\pi \le \arg z \le \frac{1}{2q}\pi \right\}$. Let λ be a root in the first group. Thus

$$\lim_{\kappa \to +\infty} \lambda = 0.$$

As $P(0) > 0$ and $Q(0) > 0$, for a large enough κ, the real parts of $P(\lambda)$ and $Q(\lambda)$ are both positive and approximately $P(0)$ and $Q(0)$, respectively. Meanwhile, the absolute values of the imaginary parts of $P(\lambda)$ and $Q(\lambda)$ are very small. Hence, the arguments of $P(\lambda)$

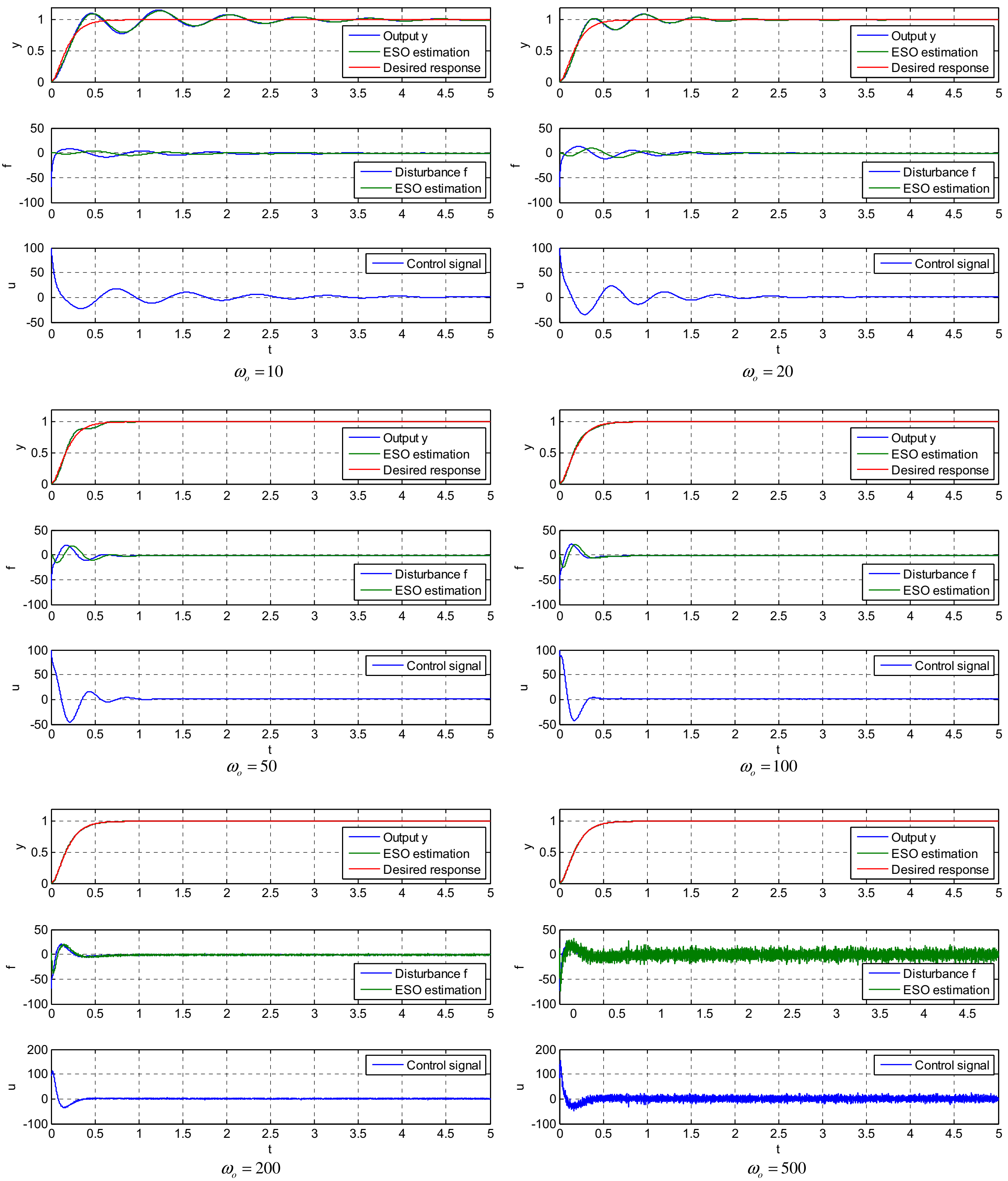

Fig. 2. System responses with different ω_o.

and $Q(\lambda)$ are almost zero such that

$$arg\frac{Q(\lambda)}{P(\lambda)} = argQ(\lambda) - argP(\lambda) \in \left(-\frac{\pi}{2}, \frac{\pi}{2}\right).$$

As $\kappa\lambda^q = -(Q(\lambda)/P(\lambda))$ and $\kappa > 0$, we can obtain

$$arg\lambda^q \in \left(-\pi, -\frac{\pi}{2}\right) \cup \left(\frac{\pi}{2}, \pi\right),$$

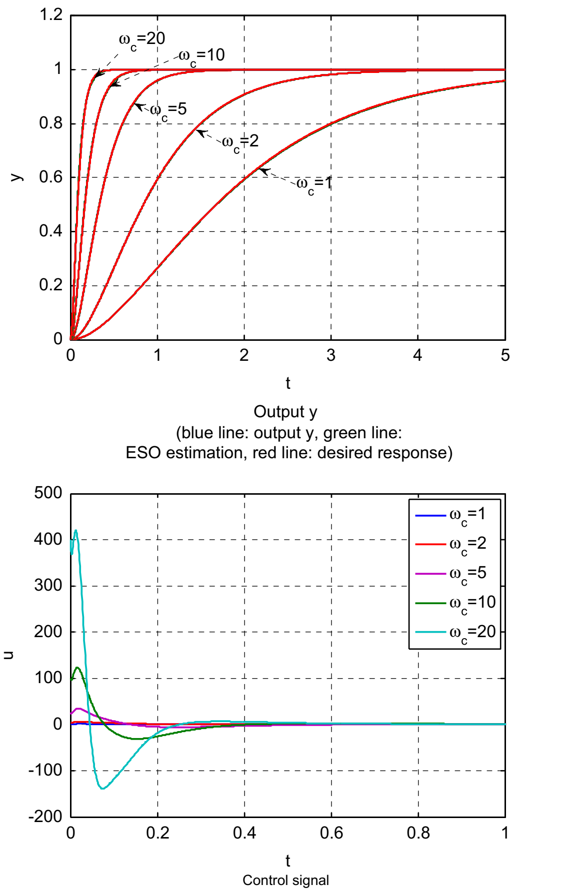

Fig. 3. System responses with different ω_c. (For interpretation of the references to color in this figure legend, the reader is referred to the web version of this article.)

indicating that $\arg\lambda^q \notin [-(\pi/2), (\pi/2)]$. Hence

$$arg\lambda \notin \left[-\frac{1}{2q}\pi, \frac{1}{2q}\pi\right].$$

Considering λ can be any of the q roots in the first group, the proof is completed.□

Lemma 2. Let us assume that the following model is open-loop stable:

$$y(s) = H(s)u(s), \tag{19}$$

where s, y, and u represent the differential operator, the output, and the control input, respectively,

$$H(s) = \frac{h_2(s)}{h_1(s)} b_0,\ \ b_0 \neq 0 \quad h_1(s) = s^{\frac{m_1}{q}} + \sum_{i=0}^{m_1-1} h_{1i} s^{\frac{i}{q}},$$

$$h_2(s) = \sum_{i=0}^{m_2} h_{2i} s^{\frac{i}{q}},\ \ h_{20} = 1,\ \ h_{2m_2} \neq 0,$$

$q > 0$, $m_1 > 0$, and $m_2 \geq 0$ are integers, and $m_1 \geq m_2$. Then, the following ADRC scheme can stabilize the closed-loop system:

$$\begin{cases} \dot{z}_1 = z_2 - \beta_1(z_1 - y) + b_e u \\ \dot{z}_2 = -\beta_2(z_1 - y) u = \frac{1}{b_e}(-z_2 + p_1(v - z_1)) \end{cases} \tag{20}$$

Proof. Based on the results in Ref. [35], the close-loop system can be expressed as

$$y(s) = G_c(s)v(s), \tag{21}$$

where

$$G_c(s) = \frac{1}{c(s)} b_v(s) h_2(s),$$

$$c(s) = \frac{b_e}{b_0} a(s) h_1(s) + b_y(s) h_2(s),$$

$$a(s) = s(s + \beta_1 + p_1),$$

$$b_v(s) = p_1(s^2 + \beta_1 s + \beta_2),$$

$$b_y(s) = (\beta_1 p_1 + \beta_2)s + p_1 \beta_2.$$

Let $\lambda = s^{\frac{1}{q}}$. Then, $c(\lambda^q)$, $a(\lambda^q)h_1(\lambda^q)$, $(1/\lambda^q)a(\lambda^q)h_1(\lambda^q)$, and $b_y(\lambda^q)h_2(\lambda^q)$ are the polynomials of λ. Further

$$deg\left(\frac{1}{\lambda^q} a(\lambda^q) h_1(\lambda^q)\right) + q = deg(a(\lambda^q)h_1(\lambda^q)) \geq deg(b_y(\lambda^q)h_2(\lambda^q)).$$

As Eq. (19) is open-loop stable, all roots of $h_1(\lambda^q)$ are outside the set $\{z | z \in C,\ -(1/2q)\pi \leq argz \leq (1/2q)\pi\}$[54].

Considering $\frac{1}{\lambda^q} a(\lambda^q) h_1(\lambda^q) = (\lambda^q + \beta_1 + p_1) h_1(\lambda^q)$, the argument of any of its root is not in the interval $[-(1/2q)\pi, (1/2q)\pi]$.

Thus, from Lemma 1, any root of $c(s)$ cannot be in the set $\{z | z \in C,\ -(1/2q)\pi \leq argz \leq (1/2q)\pi\}$ if (b_e/b_0) is large enough. As b_e is a controller parameter, the requirement can be met by choosing b_e such that $b_e b_0 > 0$ and by enlarging $|b_e|$. Hence, close-loop stability is guaranteed [54].□

Theorem 1. Assume that the following rational-order linear-time-invariant (LTI) model is open-loop stable:

$$y(s) = \frac{\sum_{i=0}^{r_2} g_{2,i} s^{\alpha_{2,i}}}{\sum_{j=0}^{r_1} g_{1,j} s^{\alpha_{1,j}}} u(s), \tag{22}$$

where $0 = \alpha_{i,0} < \alpha_{i,1} < \ldots < \alpha_{i,r_i}$ $(i = 1,2)$, $\alpha_{i,r_1} \geq \alpha_{i,r_2}$, and the real numbers $g_{1,j} > 0\,(j = 0,1,\ldots,r_1)$, $g_{2,i} > 0\,(i = 1,2,\ldots,r_2)$, $g_{2,0} = 1$. Then, Eq. (22) can be stabilized by the ADRC scheme [Eq. (20)].

Proof. As rational numbers can be expressed in fractional form, q can be set equal to the lowest common multiple of the denominators in all the powers that exist in the model transfer function. This condition means that Eq. (22) can be expressed in the form of Eq. (19). Thus, the proof is completed according to Lemma 2.□

4. Simulation result

In this section, ADRC and the fractional-order dynamics rejection scheme are used on fractional-order systems, including a

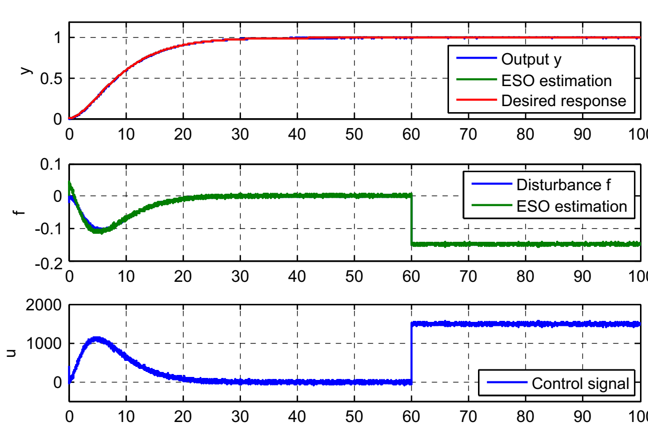

Fig. 4. Comparison of system response and ESO estimation of the heating–furnace model.

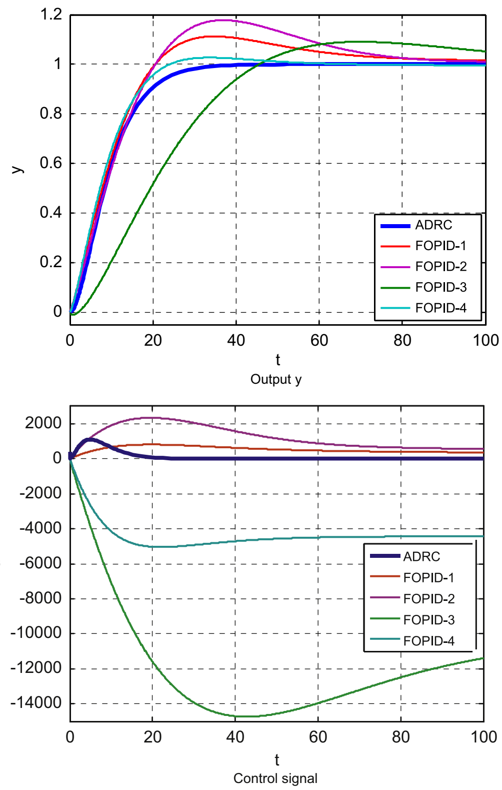

Fig. 5. Comparison of ADRC and FOPID on heating–furnace model.

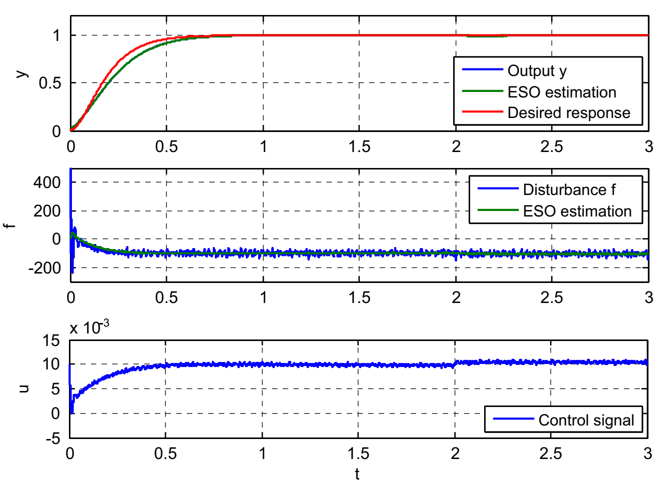

Fig. 6. Comparison of the system response and ESO estimation at 90% rated speed demand.

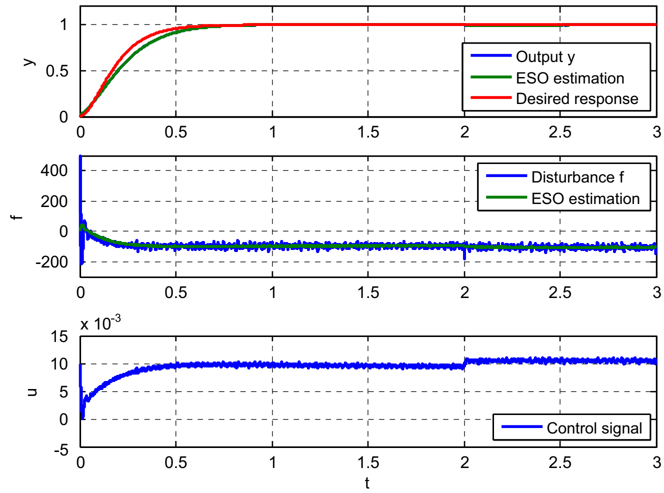

Fig. 7. Comparison of system response and ESO estimation at 93% rated speed demand.

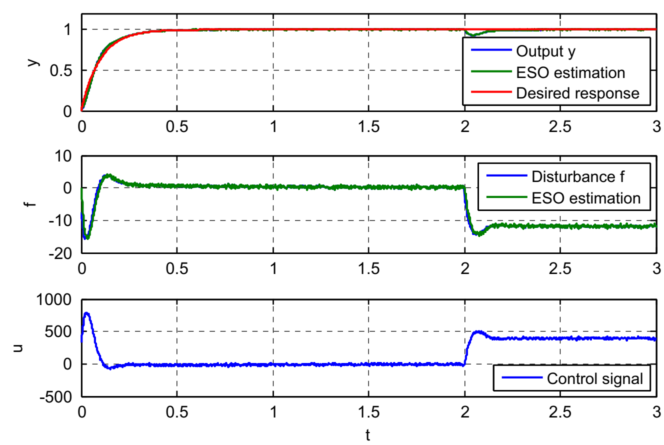

Fig. 8. Comparison of system response and ESO estimation on the heat-solid model.

Table 1
Test models and ADRC parameters.

No.	Model	ADRC parameters		
		b_e	ω_o	ω_c
1	$G_{\mathrm{I}}^1(s)=\frac{1}{0.4s^{0.5}+1}$	2.5	300	10
2	$G_{\mathrm{II}}^2(s)=\frac{1}{0.8s^{2.2}+0.5s^{0.9}+1}$	1	300	10
3	$G_{\mathrm{II}}^3(s)=\frac{1}{0.6s^{0.8}+0.9s^{0.3}+1}$	2	300	10
4	$G_{\mathrm{II}}^4(s)=\frac{1}{0.4s^{2.4}+s}$	2.5	500	10
5	$G_{\mathrm{III}}^5(s)=\frac{0.8s^{1.2}+2}{1.1s^{1.8}+0.8s^{1.3}+1.9s^{0.5}+0.4}$	2	300	10

heating–furnace, a gas–turbine, a heat solid, and some published models. Taking into consideration input disturbance w and the sensor noise, a common ADRC system is shown in Fig. 1.

4.1. Heating–furnace model

Based on a set of measured values $y_i^*(i=0,1,\ldots,M)$, Podlubny et al. identified three models of a real experimental heating furnace [3]. Among the three, the most accurate model is described by a three-term fractional differential equation, which belongs to the Type II system presented in this paper.

$$a_2y^{(\alpha_2)}+a_1y^{(\alpha_1)}+a_0y=b_0u \tag{23}$$

The parameters were obtained considering external disturbance w

$$14994.3y^{(1.31)}+6009.52y^{(0.97)}+1.69y=w+u \tag{24}$$

From the proposed approach presented in Section 3, tuning $b_e=\ 0.0001\approx b_0/a_2=1/14994.3$, $\omega_o=100000$, and $\omega_c=0.2$ is easy. External disturbance $w=-0.1$ constitutes a step signal when $t=60$ and the sensor noise is considered. The step response and control signal are shown in Fig. 4. The ESO outputs, which are the estimation of y and f, are compared with the actual y and f, respectively. The desired response is also given for comparison with y and $\hat{y}$.

Fig. 4 shows that ESO estimates y and f accurately. Output y is the same as the desired response. The fractional-order dynamics and the external disturbance are estimated and cancelled effectively, although output y is affected by the sensor noise.

To control this system, Ref. [55–58] proposed turning methods, respectively, which led to the FOPID controllers

$$C_{\mathrm{FOPID-1}}(s) = 100(s^{0.31} + 10 + s^{-0.5})$$

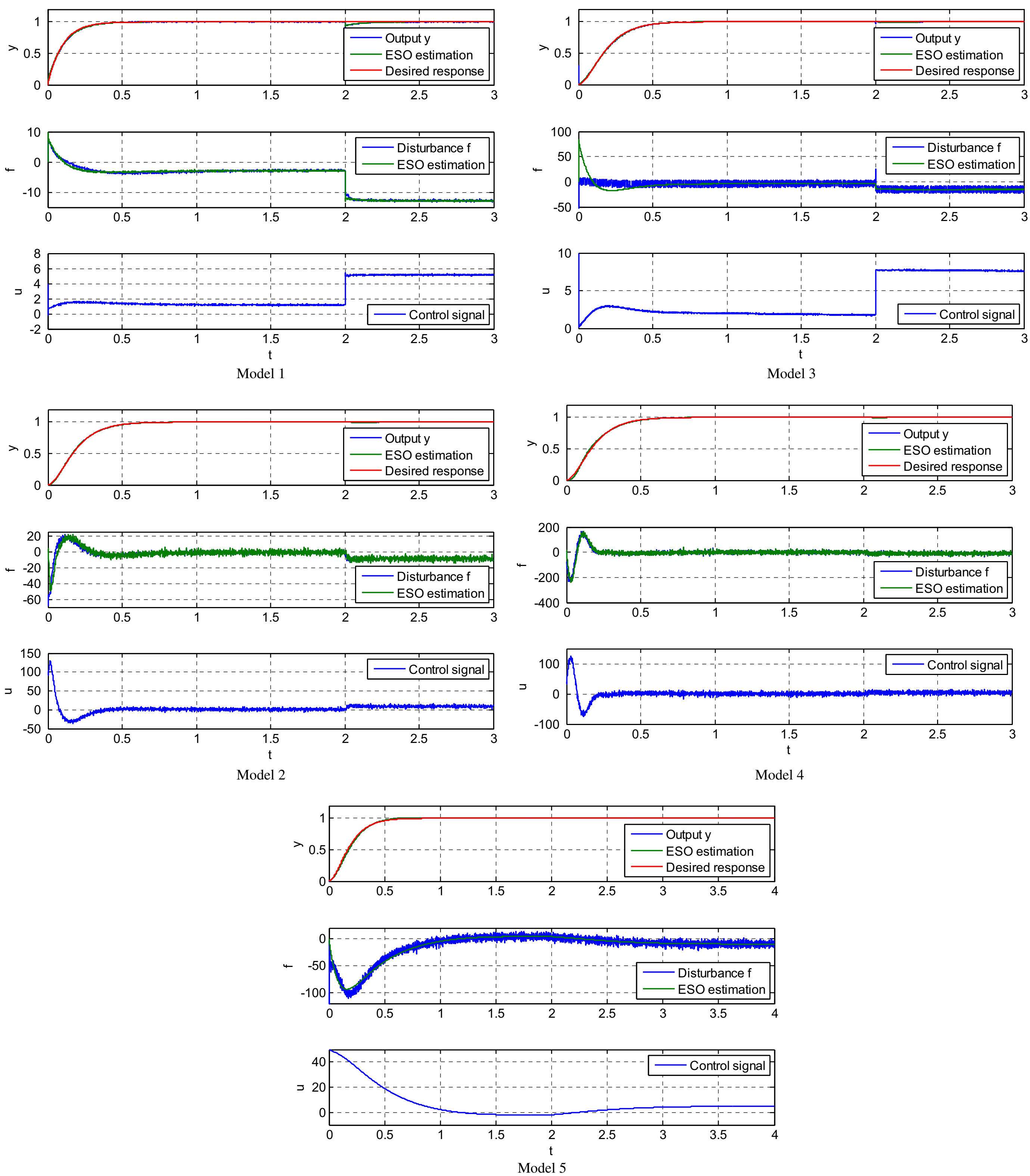

Fig. 9. Comparison of system responses and ESO estimations on hypothetical models.

$$C_{\mathrm{FOPID}-2}(s)=714.9739+\frac{107.0099}{s^{0.6}}+287.7011s^{0.35}$$

$$C_{\mathrm{FOPID}-3}(s)=736.8054-\frac{0.5885}{s^{0.6}}-818.4204s^{0.35}$$

$$C_{\mathrm{FOPID}-4}(s)=1924.7-\frac{111.8922}{s^{0.325}}-653.2185s^{0.325}$$

Fig. 5 shows the step response and control signal of ADRC and FOPID. For fair comparison, external disturbance and sensor noise are not considered.

4.2. Gas–turbine model

The fractional-order gas–turbine model is derived from the input–output operating data using the system identification method [4,5]. The input of the model is the fuel rate, and the output is the turbine speed. In general, the gas turbine is operated between 90% and 93% of the rated speed demand. The structure of this fractional-order model also belongs to the Type II system as follows:

$$G_{\mathrm{II}}(s)=\frac{b_0}{a_2s^{\alpha_2}+a_1s^{\alpha_1}+a_0} \tag{25}$$

At 90% of the rated speed demand, the fractional-order model is

$$G_{GT90}(s)=\frac{103.9705}{0.00734s^{1.6807}+0.1356s^{0.8421}+1} \tag{26}$$

Similarly, at 93% of the rated speed demand, the fractional-order model is identified as

$$G_{GT93}(s)=\frac{110.9238}{0.0130s^{1.6062}+0.1818s^{0.7089}+1} \tag{27}$$

The ADRC is tuned for 90% of the rated speed demand model. The best b_e is $(b_0/a_2)=8532.6$; thus, b_e is set as $b_e=10000$ to come up with a realistic design. ω_o and ω_c are tuned as $\omega_o=100$ and $\omega_c=10$. The external disturbance $w=-10$ constitutes a step signal when $t=2$ and sensor noise is considered. At 90% of the rated speed demand, the ESO output and the actual response are compared and shown in Fig. 6, which also shows the desired response. Fig. 7 shows the same response under the same b_e, ω_o, and ω_c when the rated speed demand changes to 93%. ESO is very effective, and output y is closed to the desired response.

4.3. Heat-solid model

A heat solid model is categorized to belong to the Type I system

$$G_{HS}(s)=\frac{1}{39.69s^{1.26}+0.598} \tag{28}$$

heated by an electrical radiator in which the temperature is measured by a pyrometer; the input and the output are voltages. Thus, the parameters are obtained using an identification method based on minimization of the quadratic criteria-difference between measured and model values [6].

For a Type I system, the first-order ADRC/second-order ESO is more suitable. Tuning $b_e=0.03\approx 1/39.69$, $\omega_o=300$, and $\omega_c=10$ is easy. The external disturbance $w=-10$ constitutes a step signal when $t=2$ and sensor noise is considered. The simulation results shown in Fig. 8 demonstrate that the first-order ADRC/second-order ESO performs well in the Type I system.

4.4. Other examples

This section includes some published fractional-order systems, which are hypothetical models [10,11,13–15]. Most are controlled by fractional-order controllers, but ADRC is used to demonstrate the effectiveness of the fractional-order dynamics rejection scheme proposed in this paper. One Type I system, three Type II systems, and one Type III system are chosen to test the ADRC tuned in Table 1. The simulation results are shown in Fig. 9. The external disturbance $w=-10$ constitutes a step signal when $t=2$ and sensor noise is considered.

Table 2
ADRC parameters and FOPID controllers.

Model	ADRC parameters			FOPID
	b_e	ω_o	ω_c	
G_{II}^2	1	1000	60	$C(s)=20.5(s^{1.2}+1)$
G_{II}^3	2	500	30	$C(s)=1.72+41.524s^{-0.668}+1.59s^{0.824}$
G_{II}^4	2.5	500	10	$C(s)=6.3092(1+0.9435s)^{1.205}$

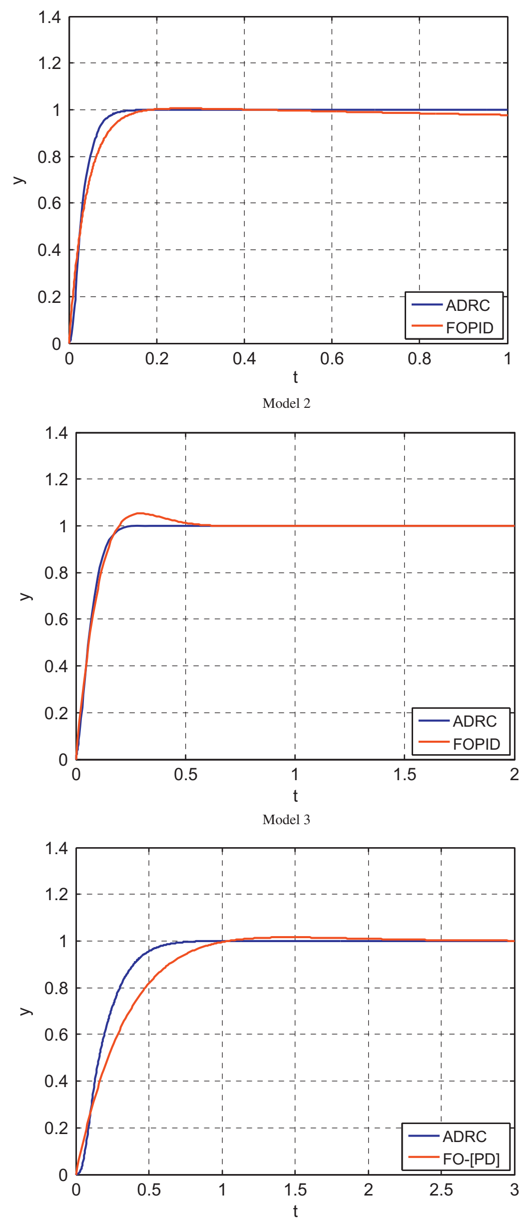

Fig. 10. Comparison of ADRC and FOPID on hypothetical models.

Adopting the same ω_c, all step responses are clearly and interestingly the same as the desired response. Although the measurement of output y is affected by sensor noise, ESO estimates y and f accurately. The external disturbance w is also estimated and cancelled. Based on ADRC, the proposed fractional-order dynamics rejection scheme is demonstrated to be effective in fractional-order systems.

Ref. [55,14,15] proposed tuning methods of FOPID to control model 2, model 3, and model 4. Table 2 gives the re-tuned ADRC parameters and FOPID controllers. Fig. 10 shows the step response of ADRC and FOPID. For fair comparison, external disturbance and sensor noise are not considered. It is clearly that ADRC is effective in fractional-order system control as FOPID.

5. Conclusions

Generally, fractional-order system is controlled by fractional-order controller. However, in this paper, a novel approach based on ADRC has been successfully applied on fractional-order systems, where fractional-order dynamics are treated as a common disturbance and actively rejected. Meanwhile, the external disturbance, sensor noise, and parameter disturbance are estimated and rejected. The stability of ADRC has been proven. The simulation test results of three physical models and five hypothetical models showed that the output was close to the desired response of ADRC. Using simple tuning parameters, ADRC can control easily fractional-order systems. Thus, ADRC is also likely appropriate in other types of fractional-order system controls.

Acknowledgment

The authors would like to thank Professor Z. Gao for his guidance on ADRC and Professor D. Xue for the simulation toolbox. The authors also would like to thank Editor Professor Y. Chen and all reviewers for their precious comments and suggestions. This research has been supported by the National Natural Science Foundation of China #51176086.

References

[1] Westerlund S. Capacitor theory. IEEE Transactions on Dielectrics and Electrical Insulation 1994;1(5):826–39.
[2] Torvik PJ, Bagley RL. On the appearance of the fractional derivative in the behavior of real materials. Transactions of the ASME 1984;51(2):294–8.
[3] Podlubny I, Dorcak L, Kostial I. On fractional derivatives, fractional-order dynamic systems and $PI^{\lambda}D^{\mu}$-controllers. In: Proceedings of the 36th conference on decision & control; 1997. p. 4985–4990.
[4] Deshpande MK. Interval methods for analysis and synthesis of linear and nonlinear uncertain fractional order systems. PhD dissertation. Mumbai, India: Indian Institute of Technology, Bombay; 2006.
[5] Nataraj PSV, Kalla R. Computation of spectral sets for uncertain linear fractional-order systems. Communications in Nonlinear Science and Numerical Simulation 2009;15(4):946–55.
[6] PETRÁŠ I, VINAGRE BM, DORČÁK ✓L, FELIU V. Fractional digital control of a heat solid: experimental results. International carpathian control Conference ICCC'; 2002. p. 365–70.
[7] Tavakoli-Kakhki M, Haeri M. Fractional order model reduction approach based on retention of the dominant dynamics: application in IMC based tuning of FOPI and FOPID controllers. ISA Transactions 2011;50(3):432–42.
[8] Das S, Pan I, Das S, Gupta A. Improved model reduction and tuning of fractional-order $PI^{\lambda}D^{\mu}$ controllers for analytical rule extraction with genetic programming. ISA Transactions 2012;51(2):237–61.
[9] Chen YQ. Ubiquitous fractional order controls? Second IFAC workshop on fractional differentiation and its applications; 2006.
[10] Chen YQ, Petras I, Xue D. Fractional order control—a tutorial. 2009 American control conference; 2009. p. 1397–411.
[11] Podlubny I. Fractional-order systems and $PI^{\lambda}D^{\mu}$-controllers. IEEE Transactions on Automatic Control 1999;44(1):208–13.
[12] Hamamci SE. An algorithm for stabilization of fractional-order time delay systems using fractional-order PID controllers. IEEE Transactions on Automatic Control 2007;52(10):1964–9.
[13] Luo Y, Chen YQ, Wang CY, Pi YG. Tuning fractional order proportional integral controllers for fractional order systems. Journal of Process Control 2010;20(7):823–31.
[14] Biswas A, Das S, Abraham A, Dasgupta S. Design of fractional-order $PI^{\lambda}D^{\mu}$ controllers with an improved differential evolution. Engineering Applications of Artificial Intelligence 2009;22(2):343–50.
[15] Luo Y, Chen YQ. Fractional order [proportional derivative] controller for a class of fractional order systems. Automatica 2009;45(10):2446–50.
[16] Li HS, Luo Y, Chen YQ. A fractional order proportional and derivative (FOPD) motion controller: tuning rule and experiments. IEEE Transactions on Control Systems Technology 2010;18(2):516–20.
[17] Luo Y, Chen YQ, Pi Y. Fractional order ultra low-speed position servo: improved performance via describing function analysis. ISA Transactions 2011;50(1):53–60.
[18] Das S, Saha S, Das S, Gupta A. On the selection of tuning methodology of FOPID controllers for the control of higher order processes. ISA Transactions 2011;50(3):376–88.
[19] Pan I, Das S, Gupta A. Handling packet dropouts and random delays for unstable delayed processes in NCS by optimal tuning of $PI^{\lambda}D^{\mu}$ controllers with evolutionary algorithms. ISA Transactions 2011;50(4):557–72.
[20] Raynaud HF, Zergainoh A. State-space representation for fractional-order controllers. Automatica 2000;36(7):1017–21.
[21] Oustaloup A. The CRONE approach: theoretical developments and major applications. In: Proceedings of second IFAC workshop on fractional differentiation and its applications; 2006. p. 39–69.
[22] Oustaloup A. CRONE control: principle, synthesis, performances with nonlinearities and robustness-input immunity dilemma. Lecture Notes in Control and Information Sciences 1990;144:767–77.
[23] Sabatier J, Oustaloup A, Iturricha AG, Lanusse P. CRONE control: principles and extension to time-variant plants with asymptotically constant coefficients. Nonlinear Dynamics 2002;29(1-4):363–85.
[24] Oustaloup A, Moreau X, Nouillant M. The CRONE suspension. Control Engineering Practice 1996;4(8):1101–8.
[25] Vinagre BM, Feliu V. Optimal fractional controllers for rational order systems: a special case of the Wiener–Hopf spectral factorization method. IEEE Transactions on Automatic Control 2007;52(12):2385–9.
[26] Feliu V, Vinagre BM, Monje CA. Fractional-order control of a flexible manipulator. Advances in Fractional Calculus: Theoretical Developments and Applications in Physics and Engineering 2007:449–62.
[27] Monje CA, Ramos F, Feliu V, Vinagre BM. Tip position control of a lightweight flexible manipulator using a fractional order controller. IET Control Theory Applications 2007;1(5):1451–60.
[28] Gao Z. Active disturbance rejection control: a paradigm shift in feedback control system design. In: Proceedings of the American control conference; 2006. p. 2399–405.
[29] Gao Z, Huang Y, Han J. An alternative paradigm for control system design. In: Proceedings of IEEE conference on decision and control; 2001. p. 4578–85.
[30] Han J. Control theory: is it a theory of model or control? Systems Science and Mathematical Sciences 1989;9(4):328–35 In Chinese.
[31] Han J. From PID to active disturbance rejection control. IEEE Transactions on Industrial Electronics 2009;56(3):900–6.
[32] Gao Z. Scaling and bandwidth-parameterization based controller tuning. In: Proceedings of the 2003 American control conference; 2003. 4989–96.
[33] Zhou W, Shao S, Gao Z. A stability study of the active disturbance rejection control problem by a singular perturbation approach. Applied Mathematical Sciences 2009;3(10):491–508.
[34] Zheng Q, Gao LQ, Gao Z. On stability analysis of active disturbance rejection control for nonlinear time-varying plants with unknown dynamics. In: Proceedings of the 46th IEEE conference on decision and control; 2007. p. 3501–6.
[35] Zhao C. Capability of ADRC for minimum-phase plants with unknown orders and uncertain relative degrees. In: Proceedings of the 2010 Chinese control conference; 2010. p. 6121–6.
[36] Tian G, Gao Z. Frequency response analysis of active disturbance rejection based control system. In: 16th IEEE international conference on control applications part of IEEE multi-conference on systems and control; 2007. p. 1595–9.
[37] Sun B, Gao ZA. DSP-based active disturbance rejection control design for a 1-kW H-bridge DC–DC power converter. IEEE Transactions on Industrial Electronics 2005;52(5):1271–7.
[38] Xia Y, Shi P, Liu GP, Rees D, Han J. Active disturbance rejection control for uncertain multivariable systems with time-delay. IET Control Theory Application 2007;1(1):75–81.
[39] Zheng Q, Gao LQ, Gao Z. On validation of extended state observer through analysis and experimentation. Journal of Dynamic Systems, Measurement, and Control 2012;134(2):024505 (6 pages).
[40] Gao Z, Hu S, Jiang F. A novel motion control design approach based on active disturbance rejection. IEEE CDC conference; 2001. p. 4877–82.
[41] Zheng Q, Gao Z. Motion control design optimization: problem and solutions. International Journal of Intelligent Control and Systems 2005;10(4):269–76.
[42] Tian G, Gao Z. Benchmark tests of active disturbance rejection control on an industrial motion control platform. In: 2009 American control conference Hyatt Regency Riverfront; 2009. p. 5552–7.
[43] Goforth FJ, Zheng Q, Gao Z. A novel practical control approach for rate independent hysteretic systems. ISA Transactions 2012;51(3):477–84.

[44] Miklosovic R, Gao Z. A dynamic decoupling method for controlling high performance turbofan engines. In: Proceeding of the 16th IFAC world congress; 2005. 16(1).
[45] Huang Y, Xu K, Han J, Lam J. Flight control design using extended state observer and non-smooth feedback. In: IEEE CDC conference; 2001. p. 223–8.
[46] Dong L, Zhang Y, Gao Z. A robust decentralized load frequency controller for interconnected power systems. ISA Transactions 2012;51(3):410–9.
[47] Zheng Q, Chen Z, Gao Z. A dynamic decoupling control approach and its applications to chemical processes. In: Proceedings of the 2007 American control conference; 2007. p. 5176–81.
[48] Zheng Q, Dong L, Lee DH, Gao Z. Active disturbance rejection control for MEMS gyroscopes. In: 2008 American control conference; 2008. p. 4425–30.
[49] Zheng Q, Dong L, Gao Z. Control and rotation rate estimation of vibrational MEMS gyroscopes. In: 16th IEEE international conference on control applications part of IEEE multi-conference on systems and control; 2007. p. 118–23.
[50] Wu D, Chen K. Design and analysis of precision active disturbance rejection control for noncircular turning process. IEEE Transactions on Industrial Electronics 2009;56(7):2746–53.
[51] Yu T, Chan KW, Tong JP, Zhou B, Li DH. Coordinated robust nonlinear boiler–turbine–generator control systems via approximate dynamic feedback linearization. Journal of Process Control 2010;20(4):365–74.
[52] Matignon D. Stability properties for generalized fractional differential systems. In: ESAIM: Proceedings fractional differential systems models methods and applications; 1998. 5:145–58.
[53] Ostrowski A. Solution of equations in euclidean and banach space. New York: Acadamic Press; 1973.
[54] Monje CA, Chen YQ, Vinagre BM, Xue D, Feliu V. Fractional-order systems and controls: fundamentals and applications. London: Springer-Verlag; 2010.
[55] Merrikh-Bayat F, Karimi-Ghartemani M. Method for designing $PI^{\lambda}D^{\mu}$ stabilisers for minimum-phase fractional-order systems. IET Control Theory and Applications 2010;4(1):61–70.
[56] Bouafoura MK, Braiek NB. $PI^{\lambda}D^{\mu}$ controller design for integer and fractional plants using piecewise orthogonal functions. Communications in Nonlinear Science and Numerical Simulation 2010;15(5):1267–78.
[57] Zhao C., Xue D., Chen Y.Q. A fractional PID tuning algorithm for a class of fractional order plants. In: Proceedings of IEEE international conference on mechatronics and automation; 2005. p. 216–21.
[58] Tabatabaei M, Haeri M. Design of fractional order proportional–integral–derivative controller based on moment matching and characteristic ratio assignment method. Proceedings of the Institution of Mechanical Engineers, Part I: Journal of Systems and Control Engineering 2011;225(18):1040–53.